MIT Open Access Articles

Black hole binary inspiral and trajectory dominance

Black hole binary inspiral and trajectory dominance

Richard H. Price,[1] Gaurav Khanna,[2] and Scott A. Hughes[3,4,5]

[1]*Department of Physics & Astronomy, and Center for Advanced Radio Astronomy, University of Texas at Brownsville, Brownsville, Texas 78520, USA*
[2]*Department of Physics, University of Massachusetts, Dartmouth, Massachusetts 02747, USA*
[3]*Department of Physics and MIT Kavli Institute, MIT, 77 Massachusetts Avenue, Cambridge, Massachusetts 02139, USA*
[4]*Canadian Institute for Theoretical Astrophysics, University of Toronto, 60 St. George Street, Toronto, Ontario M5S 3H8, Canada*
[5]*Perimeter Institute for Theoretical Physics, Waterloo, Ontario N2L 2Y5, Canada*

Gravitational waves emitted during the inspiral, plunge and merger of a black hole binary carry linear momentum. This results in an astrophysically important recoil to the final merged black hole, a "kick" that can eject it from the nucleus of a galaxy. In a previous paper we showed that the puzzling partial cancellation of an early kick by a late antikick, and the dependence of the cancellation on black hole spin, can be understood from the phenomenology of the linear momentum waveforms. Here we connect that phenomenology to its underlying cause, the spin dependence of the inspiral trajectories. This insight suggests that the details of the plunge can be understood more broadly with a focus on inspiral trajectories.

I. INTRODUCTION

During the inspiral and merger of an asymmetric black hole (BH) binary, the linear momentum that is emitted results in a reaction, a "kick," to the final merged black hole. This kick can be strong enough to eject the merged final black hole from its host active galactic nucleus. See, for example, Refs. [1–5] for recent work discussing astrophysical implications of black hole kicks. Observational confirmations of the predicted "runaway" black holes are now starting [6].

Theoretical predictions of kicks have been based largely on supercomputer numerical computations of the nonlinear equations of general relativity for black hole inspiral and merger. These codes are now capable of evolving almost any initial binary configuration. Explorations and good guesses have been made that have led to "superkick" configurations with very large ejection velocities of the final hole [7]. What is missing is a picture of the process simple enough so that physical insights can be used, as they usually are in physics. This has been a main motivation for the visualization project by the Caltech-Cornell group [8] in which "tendex and vortex" lines are used for visualization of the relativistic gravitational fields.

Here we give a simple and compelling picture of the generation of at least some aspect of kicks, a picture based on the idea that in binary inspiral main features of emission are to be understood as manifestations of the details of trajectories. What is perhaps most important about the success of this picture is that it suggests that "trajectory dominance" may be a key to a phenomenological understanding of binary inspiral emission more generally.

The remainder of this paper is organized as follows. In Sec. II we briefly review the spin-dependent kick-antikick cancellation for equatorial orbits, along with our phenomenological explanation of the cancellation and its spin dependence. Section III then looks at inspiral orbits. It is shown that the qualitative characteristics of these orbits correlate with black hole spin in a way that suggests that it is the orbital shapes that explain the different characteristics of linear momentum emission for prograde vs retrograde orbits, and for different spins. In this section it is also shown that the root of the different orbital characteristics (and hence of the kick correlation with spin and orbital direction) is the relationship of particle orbital angular momentum and angular velocity in the spacetime of a rotating hole. Section IV then "tests" the hypothesis of trajectory dominance with two classes of numerical experiments. In the first, it is shown that a Kerr particle trajectory placed in a Schwarzschild spacetime gives substantially the same gravitational wave emission as it does in the Kerr spacetime for which it is a geodesic. The second class of tests is limited to retrograde orbits in Kerr spacetimes. It is shown that the burst of radiation from retrograde orbits arises from the reversal of angular velocity of the inspiral trajectory. We discuss the implications of these results in Sec. V.

II. PHENOMENOLOGICAL EXPLANATION OF THE KICK-ANTIKICK CANCELLATION FOR QUASICIRCULAR EQUATORIAL ORBITS

During the BH inspiral-plunge merger (IPM) the gravitational wave (GW) emission carries away linear momentum, and a net linear momentum emission builds up in some direction. A strange attribute of the linear momentum was noted by Schnittman *et al.* [9] in their computational studies of the IPM of comparable mass BHs, with spin angular momentum perpendicular to the orbital plane (This strange attribute had been predicted about a year earlier by Damour and Gopakumar [10]). The net linear momentum in some direction would grow during the inspiral phase and

then start to decrease at the plunge. For certain models the decrease removed most of the momentum emitted earlier. Subsequently, Sundararajan *et al.* [11] studied the phenomenon further with the flexibility and efficiency of particle perturbation techniques. Their results, for "particles" orbiting in the equatorial plane of a spinning black hole, included models in which 97% of the kick was cancelled by a late term antikick. It was noted in these studies that the extent of cancellation is strongly correlated with black hole spin and strongly dependent on whether the orbital motion is prograde (orbital and spin angular momentum aligned) or retrograde (antialigned). We shall call this puzzling cancellation, along with its dependence on the orbit and the BH spin, the "cancellation phenomenon."

This phenomenon was somewhat a paradox. The early momentum emission comes from the nearly Newtonian gradual inspiral, while the late emission is from the plunge and the quasinormal ringing of the merger. It seemed remarkable that the early process could somehow "set up" the late process to generate just the right amount of linear momentum so that for some models the late momentum emission almost completely canceled the early emission.

As is so often the case for an "impossible" coincidence, the explanation turns out to be simple, at least at one level. For prograde orbits the component of linear momentum flux in any direction, let us say the $\dot{P}_x$ in the x direction, is an oscillating quantity. This oscillating quantity starts with negligible amplitude in the distant past, in effect at time $t = -\infty$; it ends with zero amplitude at $t = +\infty$, when the quasinormal ringing dies out. Thus, as a function of time, $\dot{P}_x$ is an oscillation inside a modulation envelope that starts and ends at zero, and it is largest around the plunge.

The net momentum P_x radiated up to some time t is the integral of $\dot{P}_x$ from early time up to time t. The total P_x radiated for the entire IPM process, $\int_{-\infty}^{\infty} \dot{P}_x dt$ is the integral of an oscillating quantity. In that integral, the positive phases and negative phases of the oscillation will tend to cancel. Because of the changing amplitude of the oscillations the cancellation will not be complete; some net momentum can be radiated. The more rapidly the amplitude changes, the larger the result for the total momentum radiated. The total momentum in fact is easily shown to be a decreasing function of the characteristic time scale for the change in the amplitude divided by the characteristic
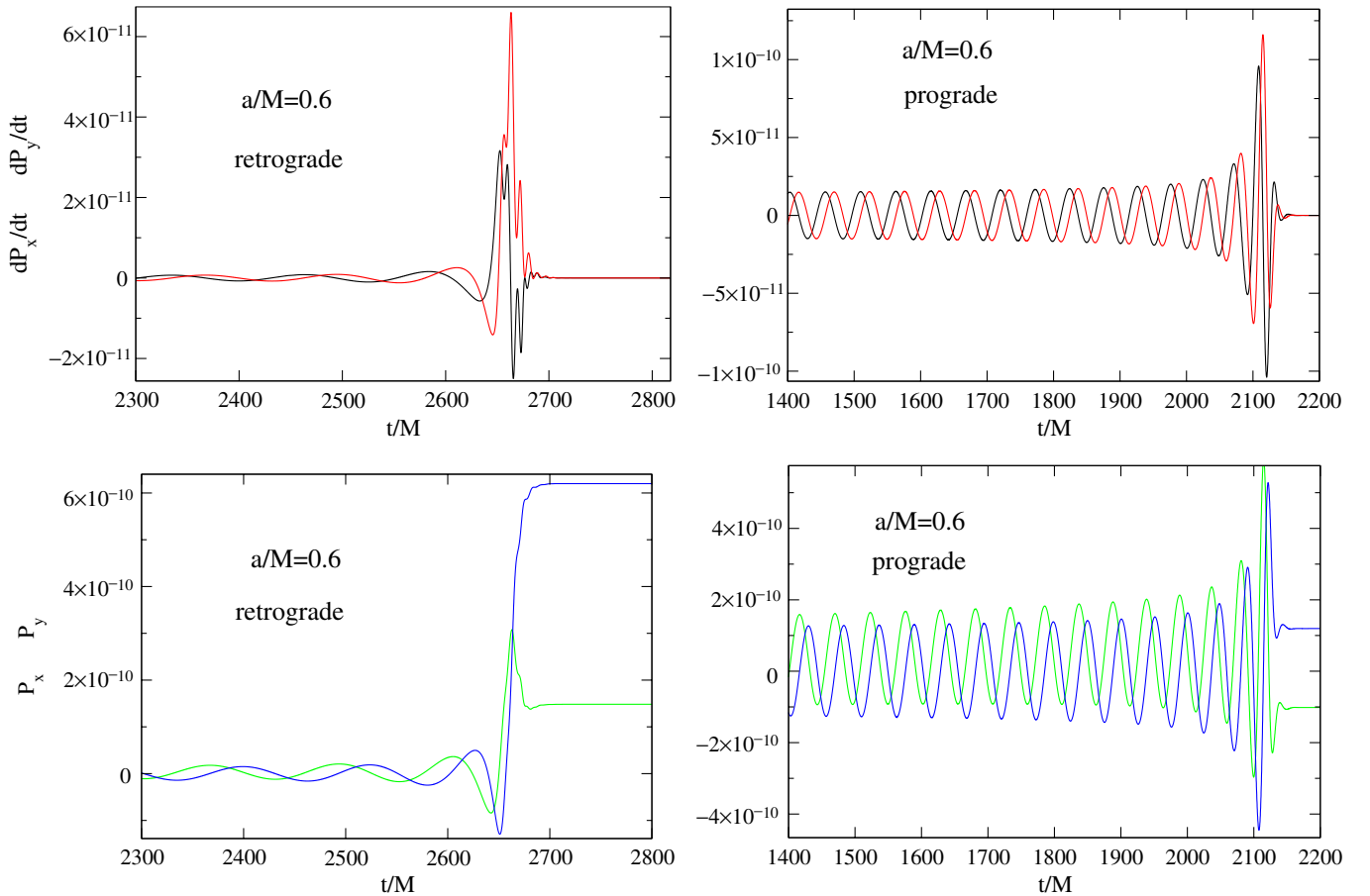

FIG. 1 (color online). The top row shows, as a function of time, the momentum flux components $\dot{P}_x$ and $\dot{P}_y$ for both a retrograde (left plot) and a prograde (right) inspiral into the $a/M = 0.6$ spinning hole. The bottom row shows the components P_x, P_y of the total linear momentum radiated from $t = -\infty$.

period of the oscillations. (For details see Ref. [12], hereafter Paper 1.)

For a very slowly varying amplitude, the components of net momentum radiated (and hence of the net kick) $\int_{-\infty}^{\infty} \dot{P}_k dt$ must be very small. Any net momentum radiated in the early increasing amplitude part of the process must be canceled in the later part. This is not a consequence of any feature of curved spacetime, but of simple mathematics. The phenomenological explanation of the cancellation phenomenon fits the results of the computations both for comparable mass BHs and for extreme mass ratio inspirals (EMRIs); the more gradually the amplitude changes, the greater is the extent to which the late antikick cancels the earlier kick. In the case of prograde equatorial orbits in EMRIs, a more definitive statement can be made. The rate of change of the envelope depends on the spin of the BH. Larger spin BHs show more slowly varying amplitudes of momentum flux, and show a more nearly complete cancellation of early and late linear momentum. Retrograde equatorial orbits show the opposite correlation: for the most rapidly spinning holes the linear momentum flux oscillations have the most rapidly changing amplitude.

Figures 1 and 2 illustrate the connection between radiated linear momentum, BH spin, and direction (prograde vs retrograde) for equatorial orbits. In the top row of each of these figures the flux of linear momentum is shown in two arbitrary orthogonal directions x, y in the asymptotically flat spacetime. In Fig. 1 the plots on the left hand side correspond to a retrograde IPM. For these retrograde cases the plots shows that the linear momentum emission is largely concentrated in a burst. The net linear momentum components (bottom row) grow suddenly upon emission of this burst, and the final linear momentum is of order of the momentum flux times the oscillatory time scale. The plots on the right, for a prograde orbit, tell a very different story. Here the momentum flux is oscillatory inside an amplitude envelope that is moderately smooth. The net momentum emitted (lower plot) is oscillatory until the amplitude peak, at which time a net momentum is built up, but—unlike the retrograde case—this net momentum is an order of magnitude less than the product of the momentum flux and an oscillatory time scale. The features shown in Fig. 1 for $a/M = 0.6$ are also present in Fig. 2 for $a/M = 0.9$, but are significantly more pronounced. For $a/M = 0.9$, the jump in radiated momentum is more sudden than for $a/M = 0.6$ in the case of the retrograde orbit, and the cancellation of the radiated momentum is
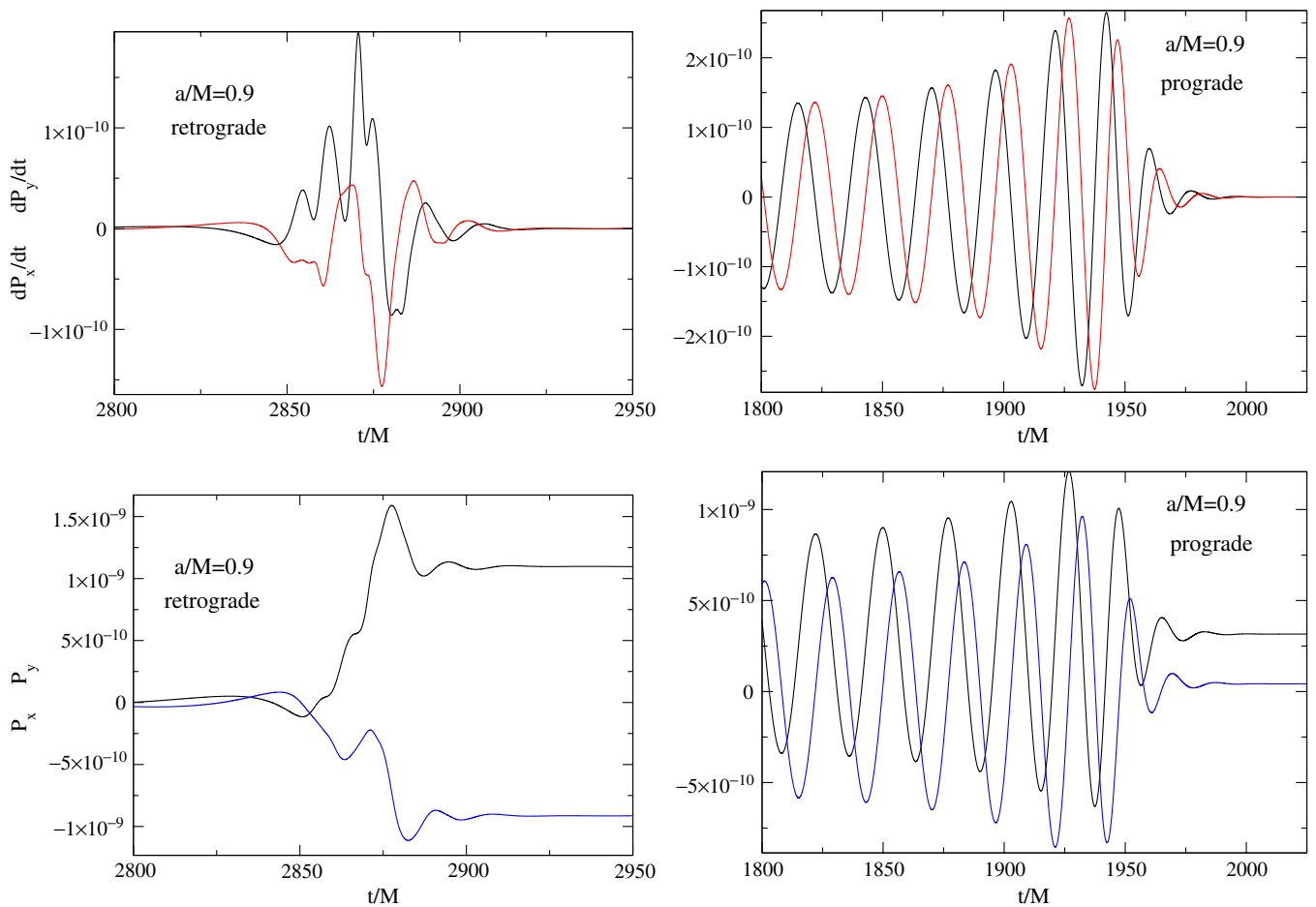

FIG. 2 (color online).　The same quantities as in Fig. 1 but here for retrograde and prograde orbits into a black hole with $a/M = 0.9$.
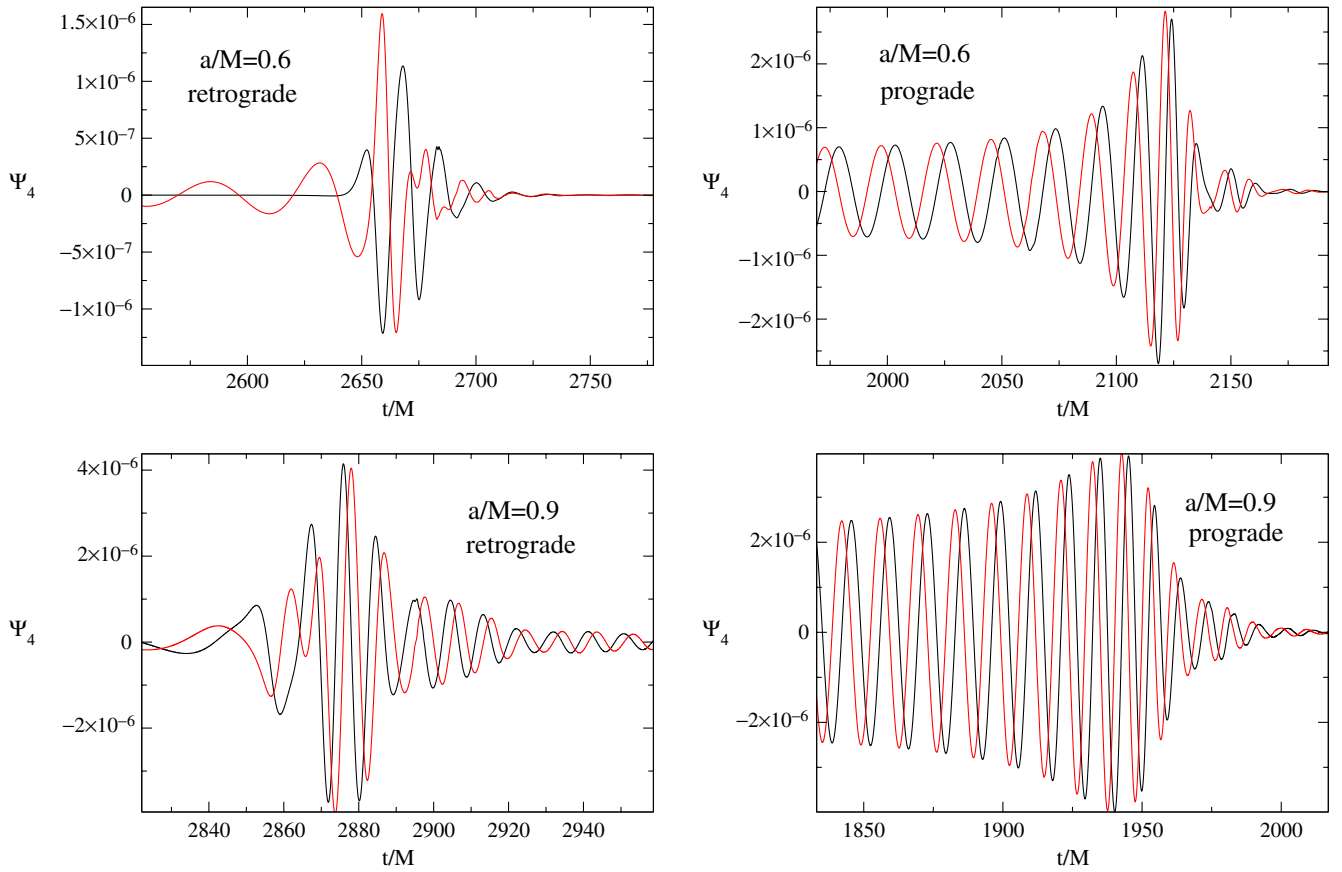
FIG. 3 (color online). Waveforms, i.e., the real and imaginary parts of the $m = 2$ component of the Teukolsky function Ψ_4 for prograde and retrograde orbits into Kerr holes with $a/M = 0.6$ and 0.9.

more nearly total than for $a/M = 0.6$ in the case of the prograde orbit.

In seeking an explanation for this cancellation, an important technical question must be asked. Linear momentum cannot be generated in a single multipole mode. Its emission therefore depends on delicate amplitude and phase relations of different modes (in fact, the relations of even modes with odd modes). We must ask whether the BH spin dependence and the very different patterns for retrograde and prograde orbits are the results of subtly shifting mode interactions, or whether they are embedded more robustly in the gravitational wave emission.

This question is answered in Fig. 3. Here the $m = 2$ part of the Teukolsky function Ψ_4 is shown for retrograde and prograde orbits for both $a/M = 0.6$ and $a/M = 0.9$. It is clear in these figures that what is seen in the linear momentum flux is also true for the gravitational waves themselves: For retrograde orbits the wave emission comes in a burst, while for prograde emission the emission is a smoothly modulated oscillation, and these characteristics increase with increasing values of a/M.

We emphasize that the observations above are phenomenological and hence our explanation in Paper I of the kick/antikick cancellation is a phenomenological one, one that is clearly compelling, but that does not really *explain* the

cancellation, since it does not explain why the prograde orbits have slowly changing oscillations and the retrograde orbits have rapidly changing oscillations. We offer such an explanation in this paper, and hence show the underlying physical explanation of the linear momentum cancellation phenomenon.

III. INSPIRAL ORBITS

The core of our explanation lies in the fact that a rotating hole drags the spacetime along with it. In the Schwarzschild spacetime, the angular velocity $d\phi/dt$ of a particle of mass μ is proportional to L, the particle's specific angular momentum (p_ϕ/μ), a constant of the motion. In the Kerr spacetime, however,

$$\frac{d\phi}{dt} = \frac{L(1 - 2M/r) + 2EMa/r}{E(r^2 + a^2 + 2Ma^2/r) - 2LMa/r}, \quad (1)$$

where E is the particle's specific energy $(-p_0/\mu)$, another constant of the motion. Because of the terms linear in a in this expression, a particle with no angular momentum can be rotating, i.e., can have nonzero $d\phi/dt$. It is of particular interest that for a particle with a nonzero L that has a sign opposite to that of a, the numerator of Eq. (1) can vanish and, since the two canceling terms have different r

dependences, can change sign as the particle moves inward. In short, the angular velocity can reverse direction.

It should be noted that the angular velocity $d\phi/dt$ here is based on the Boyer-Lindquist azimuthal angle ϕ. With another choice of the mixing of ϕ and t, the angular velocity of geodesics would be different. For this and other reasons, our arguments here are qualitative, rather than quantitative. More specifically, we note that the qualitative nature of the orbits and of the radiation are correlated. As the coordinate-dependent orbit winds more gradually, the coordinate-independent pattern of radiation is more gradually modulated. Without being too specific about the meaning of "reasonable," we believe that any reasonable choice of coordinates must show the same qualitative features as those given in Boyer-Lindquist coordinates.

This reversal is clear in Fig. 4. The figure presents the equatorial orbits for particles in Kerr spacetimes with various values of the spin parameter a/M. Positive numbers are for prograde infall (same sign for L and a), and negative numbers are for retrograde orbits (opposite signs for L and a). The plots treat the Boyer-Lindquist [13] r and ϕ coordinates of Kerr spacetime as if they were two-dimensional polar coordinates in flat spacetime. The dark outer band in each case indicates the particle orbiting many times near the radius R_{ISCO} of the innermost stable orbit (ISCO). The empty circle at the center of each panel indicates the radial coordinate location r_{hor} of the horizon. It should be noticed that both the ISCO and the horizon have different coordinate radii in different panels since these radii depend on the BH spin for a hole given mass M

(note the scales in use in different panels). The ISCO radius is quite different for prograde and for retrograde orbits.

The trajectories are not particle geodesics. The results here use the same radiation reaction modeling as in Ref. [11]. For a particle of mass μ moving in the space-times of mass M, the loss of orbital energy and angular momentum are second order in μ/M. It is assumed that these losses are slow enough that the orbits can be described as geodesics in which the particle energy and angular momentum decrease slowly in accord with radiative losses. For all models reported in the current paper, the mass ratio is $\mu/M = 10^{-4}$, so that the assumption of a slow rate of change is justified.

Because of this radiation reaction, the particle gradually spirals inward from the ISCO. Once it has been driven well off the ISCO, the radiation reaction is unimportant. Following a short transition from the earlier adiabatic inspiral [14,15], the motion is negligibly different from an infalling geodesic as the particle moves inward on a spiral that ends at the horizon. This motion is associated with the GW emission at $t \rightarrow \infty$.

It is striking in Fig. 4 that the particle moving in the prograde direction into the $a/M = 0.9$ hole orbits many times and slowly moves inward. This characteristic is less dramatic in the $a/M = 0.3$ case. The tendency is yet less in the $a/M = 0$ case, the orbit for a Schwarzschild hole. For the retrograde orbits, quite the opposite applies; as the BH spin magnitude increases, the orbit becomes less and less dominated by circumferential motion and more and more by radial motion.
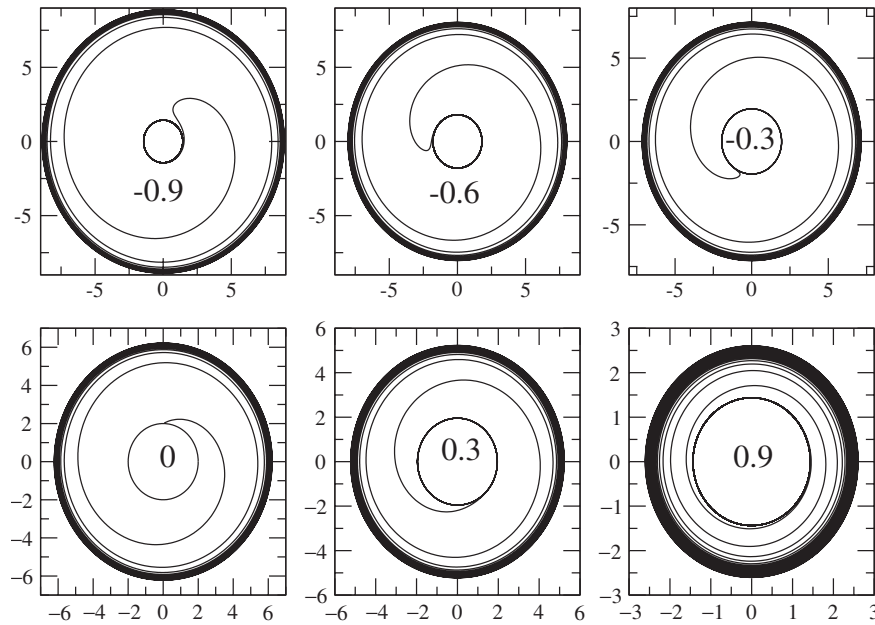

FIG. 4. Plots of the equatorial particle orbits in the Kerr geometry. Each panel is marked with the spin parameter a/M. Negative numbers indicate a retrograde orbit; positive numbers a prograde orbit. The plots treat the r and ϕ Boyer-Lindquist coordinates as if they were polar coordinates in flat two-dimensional space. The axes show the $x = r\cos\phi$ and $y = r\sin\phi$ Cartesian-like coordinates based on the Boyer-Lindquist coordinates and are given in units of the BH mass M.

A simple quantitative exploration of this correlation is possible. Since the radiation reaction at and interior to the ISCO is much smaller than the secular gravitational forces (i.e., since the trajectories are negligibly different from geodesic orbits), it is a good approximation to set the L and E parameters for infall to be those at the ISCO. These are known to give a ratio [16]

$$\frac{L}{E} = \pm \frac{M^{1/2}(r^2 \mp 2aM^{1/2}r^{1/2} + a^2)}{r^{3/2} - 2Mr^{1/2} \mp aM^{1/2}}, \qquad (2)$$

where the upper sign refers to prograde orbits and the lower to retrograde. With this ratio put into Eq. (1) we can find, for retrograde orbits, the approximate radial location r_{turn} at which $d\phi/dt$ changes sign during the plunge. These locations are presented, as functions of a/M in Fig. 5 along with radial locations of the ISCO and the horizon.

If the angular velocity reversal occurs too close (in some sense) to the horizon, gravitational redshift effects dominate to suppress outgoing gravitational wave energy and momentum. A crude index of the importance of the angular velocity reversal is therefore the ratio of the reversed-motion radial span $r_{\text{turn}} - r_{\text{hor}}$ to the full radial span $r_{\text{ISCO}} - r_{\text{hor}}$. This ratio is shown, for retrograde orbits, in Fig. 6. The implications of Fig. 4 are supported by the results in this figure; the importance of the angular velocity reversal for retrograde infall increases dramatically with an ncreasing BH spin.

We have so far focused on the retrograde orbits, while it had been the high spin prograde orbits, that produced the most interesting cancellation phenomenon. We now understand this to be due to the gradual orbiting for prograde cases after the particle has detached from the ISCO and is spiraling in toward the horizon. This gradual spiraling is particularly clear for the prograde inspiral with $a/M = 0.9$ shown in Fig. 4. A suggestion of the physical basis for this can be seen in Eq. (1): for prograde orbits, in which L and a

FIG. 6. For retrograde inspiral, the fraction of ISCO to the horizon radius for which the angular velocity is reversed. Here Δr_{turn} is $r_{\text{turn}} - r_{\text{hor}}$, the radial distance from the turning point to the horizon, and Δr_{ISCO} is $r_{\text{ISCO}} - r_{\text{hor}}$, the radial distance from ISCO to the horizon.

have the same sign, the two terms in the numerator of $d\phi/dt$ have the same sign, while for retrograde orbits they would have opposite signs. This suggests that $d\phi/dt$ is larger in the prograde case and that it increases with increasing BH spin.

The situation is actually rather more complicated. For one thing, $d\phi/dt$ for the inspiral depends on the radius; the particle whirls faster (as measured in coordinate time) as it approaches the horizon. This is shown in Fig. 7, along with the dependence of the angular velocity on a/M. We should not lose sight of the fact that $d\phi/dt$ by itself does not really determine the kick/antikick cancellation. Rather, the important point is the way in which the amplitude of the linear momentum flux changes slowly for particle motion after the plunge, i.e., inside the ISCO. Figure 7 is therefore only mildly suggestive of the reason for the increase in cancellation with increasing a/M.
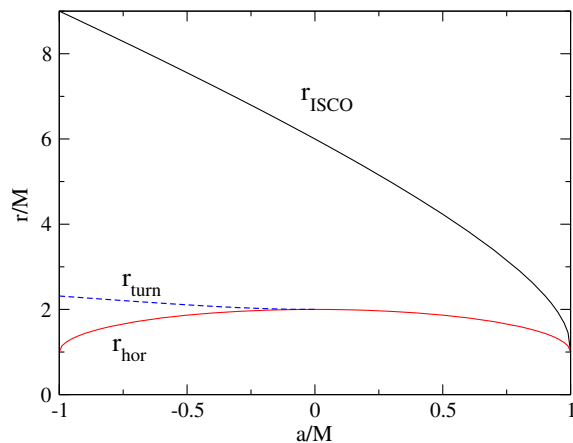

FIG. 5 (color online). The radial locations of the ISCO, horizon, and turning point are plotted as functions of the dimensionless spin parameter a/M. The turning point exists only for negative values of a/M, i.e., for retrograde orbits.
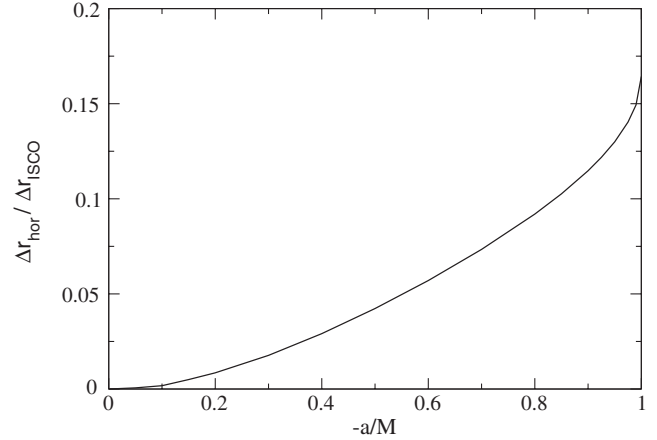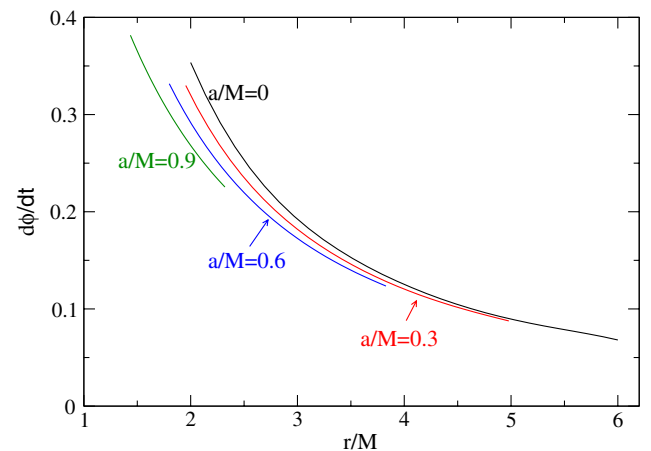

FIG. 7 (color online). The values of the particle angular velocity $d\phi/dt$ as it spirals from the ISCO to the horizon.

IV. TESTS OF THE ORBIT-DOMINANCE EXPLANATION

A. Kerr orbits embedded in Schwarzschild spacetime

Here we test the hypothesis that the nature of the kick, and of gravitational wave emission more generally, is dominated by the nature of the trajectory, rather than by the nature of the spacetime in which the gravitational waves are generated and through which they propagate. One way of investigating what dominates, trajectory or spacetime, is to take a trajectory from, say, spacetime A, put it as a source in spacetime B, and see whether the emerging radiation is characteristic of the trajectory or the spacetime. This procedure amounts to putting into spacetime B an orbit that differs dramatically from a geodesic orbit in spacetime A. This configuration, then, cannot be considered to be the extreme mass ratio limit of a process in general relativity. Nevertheless, it is mathematically consistent in linear particle perturbation theory, since the specification of the source in such calculations is an independent step.

The results of tests of this type are shown in Figs. 8 and 9. The plots show the components dP_x/dt and dP_y/dt of gravitational wave momentum flux from equatorial Kerr orbits placed in a Schwarzschild spacetime. In principle, one can start with the Kerr trajectory for a hole of mass M and nonzero spin parameter a/M. One then uses the coordinate functions $r(t)$ and $\phi(t)$ in Boyer-Lindquist coordinates as the specification of an orbit in the Schwarzschild geometry of the same mass M. In practice, this procedure encounters a problem at the horizon, since the radial location of the Kerr horizon $r = M + \sqrt{M^2 - a^2}$ is less than the radial position $2M$ for the Schwarzschild geometry. The Kerr trajectory coordinate specification would therefore extend inside the horizon in the Schwarzschild geometry.

This problem is avoided by matching not the radii of the two inspiral trajectories but rather their values of the function $\Delta_a = r^2 - 2Mr + a^2$. Given a trajectory $[r_K(t), \phi(t)]$ in the Kerr geometry, we map this to a trajectory $[r_S(t), \phi(t)]$ by requiring that $\Delta_a(r_K) = \Delta_0(r_S)$ at each moment t. In this way the horizon location (at $\Delta = 0$) of
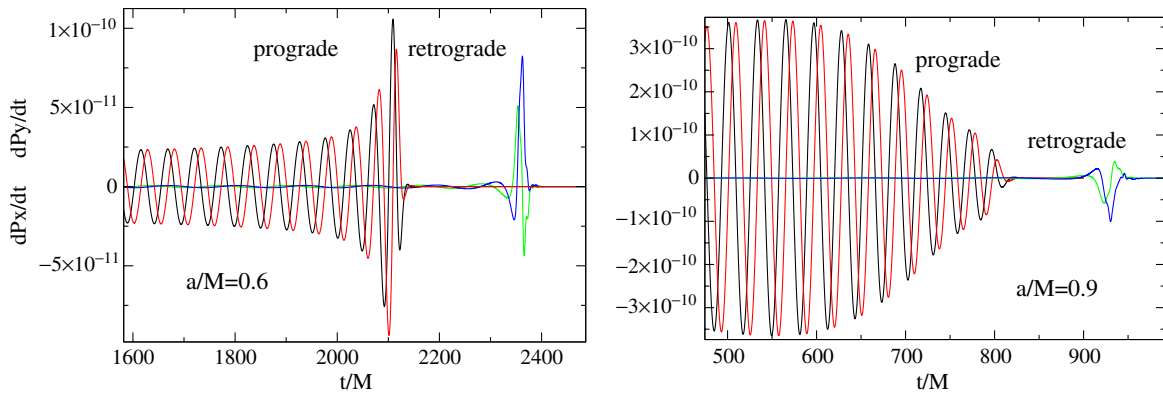

FIG. 8 (color online). The two components of momentum flux generated by Kerr inspiral orbits placed in a Schwarzschild background. The plots on the left show trajectories for $a/M = 0.6$; those on the right correspond to $a/M = 0.9$. (Note the different scales on the two plots; the amplitude of the retrograde burst for $a/M = 0.9$ is slightly higher than that for $a/M = 0.6$.).
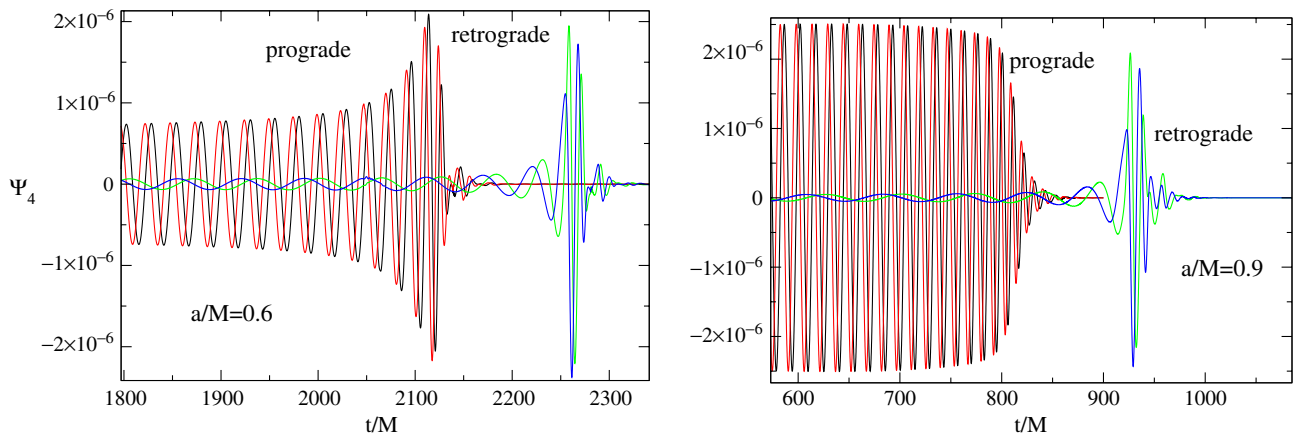

FIG. 9 (color online). The real and imaginary parts of the $m = 2$ component of the Teukolsky wave function Ψ_4 from Kerr inspiral orbits placed in a Schwarzschild background. The plots on the left show trajectories for $a/M = 0.6$; those on the right correspond to $a/M = 0.9$.

one spacetime corresponds to the horizon (at $\Delta = 0$) in the other. Though this is not the unique way of mapping the coordinate ranges, it is the simplest and most direct way. Any other way should make little difference far from the horizon and no difference at the horizon. Any smooth mapping of the coordinates will therefore give the same qualitative orbit.

The resulting plots, shown in Figs. 8 and 9, strongly support the notion of trajectory dominance. Figure 8 shows the momentum flux components from $a/M = 0.6$ and $a/M = 0.9$ orbits embedded in the Schwarzschild spacetime. For both spins there is a dramatic difference between the prograde and the retrograde momentum fluxes. A comparison of Fig. 8 with Figs. 1 and 2 shows, moreover, that the qualitative nature of the momentum emission from any of the Kerr orbits in Schwarzschild is the same as that in the Kerr spacetime in which the orbits are approximate geodesics. Figure 9 makes the same comparison for the gravitational waves, in particular for the $m = 2$ component of the Teukolsky function Ψ_4. Again, the gravitational wave emission for prograde orbits are dramatically different from retrograde orbits, and the emission is qualitatively the same for a Kerr orbit in the Schwarzschild spacetime as it is in the spacetime in which it is an approximate geodesic.

We have computed many additional examples of the radiation from a geodesic trajectory of one spacetime embedded in another spacetime. In particular, we looked at the radiation from the $r(t)$, $\phi(t)$ of a retrograde orbit embedded as a prograde orbit in a spacetime with the same BH a/M, and vice versa. In all cases, the results were minor variations of the results in Figs. 8 and 9: the radiation pattern is determined by the trajectory.

B. Correlations of timing and angular direction

As a very different test of trajectory dominance we look for features of the emerging radiation that can be correlated with features of the orbits. In particular, a strong argument for trajectory dominance was made in Sec. III based on the postplunge reversal of angular velocity for retrograde orbits. Here we look at evidence that the burst of gravitational radiation, and especially of linear momentum, from retrograde orbits really does come from that reversal event.

The results, shown Figs. 10–12 compare features of the orbit, in the left two panels, with results, in the right panels, for momentum flux observed at a Boyer-Lindquist radius of $200M$. In Fig. 10, for the retrograde inspiral orbit into a Kerr BH with $a/M = 0.9$, the left panel repeats the corresponding panel in Fig. 4, showing a picture of the trajectory and showing the angular velocity reversal occurring fairly close to the horizon. The plots of azimuthal angle ϕ and angular velocity $d\phi/dt$ confirm that reversal takes place around $\phi = 80°$, and indicate that this occurs at coordinate time $t \approx 2800M$. The plot of $1/(dt/d\tau) = 1/\gamma$ shows the relationship of coordinate time and particle proper time, and hence shows the development of the redshift factor γ. The story told by these plots then is that the relativistic effects increase after the plunge, are fairly strong around the time of angular reversal, and show the subsequent redshifting away as the particle asymptotically disappears in the horizon.

The right panel shows features of the linear momentum flux from this orbit. The plot of momentum fluxes (as in Fig. 2) show that the burst of linear momentum, starting around $t = 3000M$ is in reasonably good time agreement with the time of orbital angular velocity reversal at $t = 2800M$, when allowance is made for propagation time to the observation radius $r = 200M$.

The right panel also presents $\arctan(\dot{P}_y/\dot{P}_x)$, which gives an estimate of the direction in which the linear momentum is radiated. The direction of the momentum differs substantially from the angle at which the reversal of the angular velocity takes place. This is not too surprising, bearing in mind that due to frame dragging and strong-field
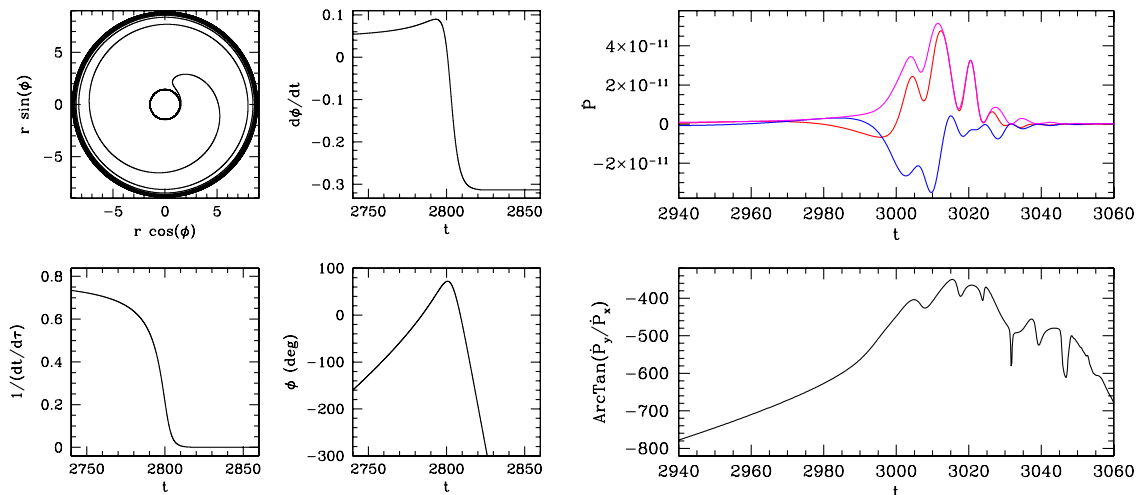

FIG. 10 (color online).   Trajectory and flux for the retrograde inspiral into a Kerr BH with $a/M = 0.9$. See text for details.
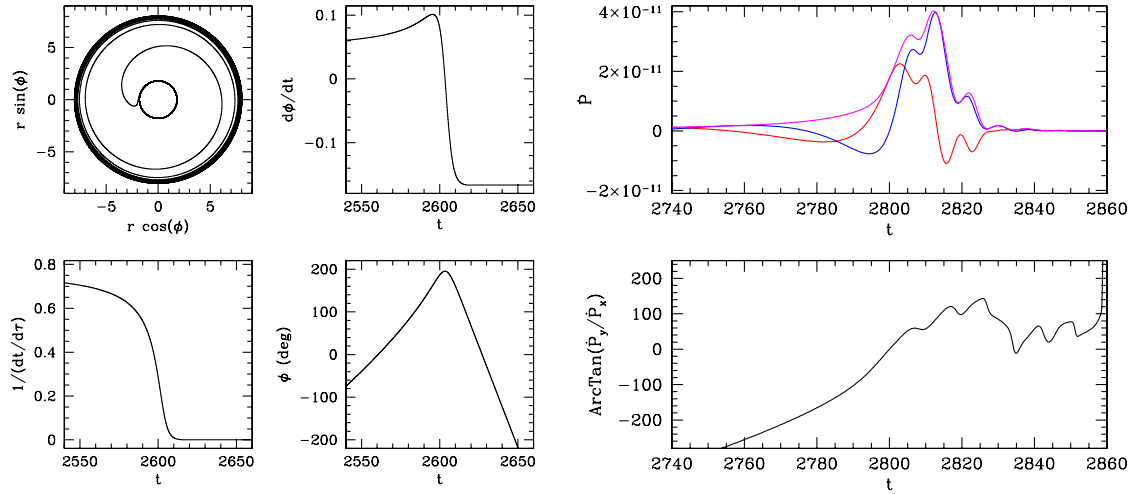
FIG. 11 (color online).   Trajectory and flux for the retrograde inspiral into a Kerr BH with $a/M = 0.6$. See text for details.
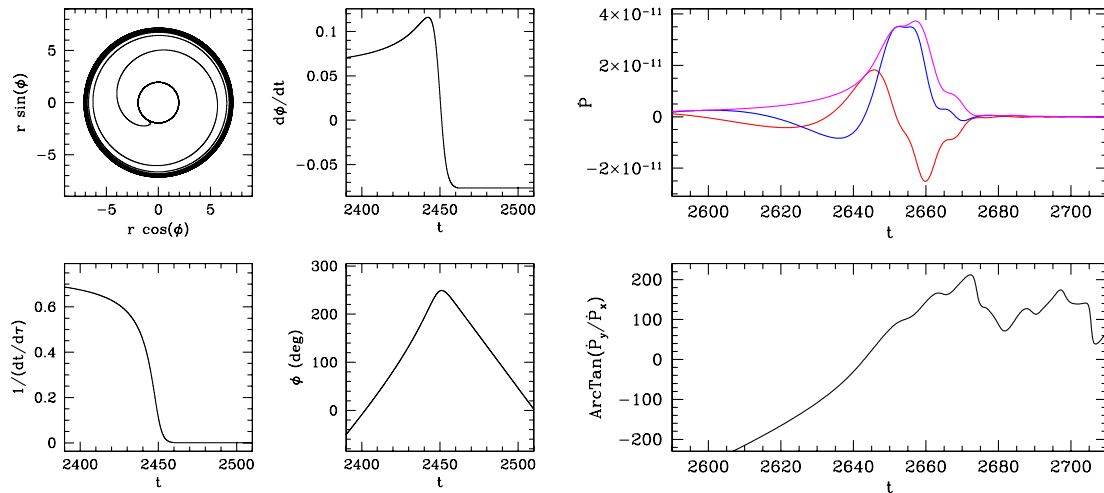

FIG. 12 (color online).   Trajectory and flux for the retrograde inspiral into a Kerr BH with $a/M = 0.3$. See text for details.

propagation effects the radiation does not proceed outward in a constant ϕ direction. What is telling is the time development of the angle of the radiated momentum. That angle increases monotonically to $t \approx 3000M$, which mirrors (with an appropriate shift) the time at which the reversal occurs. Beyond this, the angle associated with the flux is roughly constant or even decreasing (bearing in mind that the flux decays rapidly, and this angle is likely to be dominated by numerical noise as we go forward in time).

Figures 11 and 12 show analogous results for the retrograde inspiral into holes of $a/M = 0.6$ and 0.3. The discussion of the $a/M = 0.9$ case applies to these as well. The only differences are in a few of the details.

V. CONCLUSION

For particles in BH spacetimes, the spacetime itself has two effects: it determines the trajectories of the particles, and it governs the radiation emerging from the motion of those particles. We have given evidence, evidence that we consider compelling, that it is the trajectories that are crucial to the nature of the emerging radiation. The case was built in Secs. III and IV. In those sections it was argued that aside from determining the particle trajectories, the main role of the structure of the spacetime *per se* is to cut off the particle generated radiation as the particle asymptotes to the horizon. We have seen that especially in Figs. 10–12.

Although the work reported in this paper was originally motivated by a phenomenon of prograde orbits, the kick/antikick cancellation, it turns out that it is the retrograde orbits that are the more interesting and provide the strongest evidence for the dominant role of the particle orbits. This is due, in particular, to the angular velocity reversal, a feature of the orbit that can be directly connected to the pattern of radiation.

An interesting working hypothesis is that in a broader class of IPM models the radiation from a particle in a BH background can usefully be broken down into

spacetime → trajectory → radiation in which the space-time plays a role in the last step only through the horizon cutoff. Although such a simplifying picture is most applicable to the EMRI limit, we note that the kick/antikick cancellations exhibited for comparable mass holes in the work of Schnittman *et al.* [9] indicate that this picture must be at least partially applicable for comparable mass holes.

We are now using the idea of trajectory dominance to look for a deeper understanding of the generation of radiation during the plunge, the most important epoch of the IPM, but the epoch that is most difficult to treat with simple approximations.

ACKNOWLEDGMENTS

[1] M. Volonteri, K. Gültekin, and M. Dotti, Mon. Not. R. Astron. Soc. **404**, 2143 (2010); arXiv:1001.1743.

[2] O. Zanotti, L. Rezzolla, L. Del Zanna, and C. Palenzuela, Astron. Astrophys. **523**, A8 (2010).

[3] J. Guedes, P. Madau, L. Mayer, and S. Callegari, Astrophys. J. **729**, 125 (2011); arXiv:1008.2032.

[4] D. Sijacki, V. Springel, and M. Haehnelt, arXiv:1008.3313 [Mon. Not. R. Astron. Soc. (to be published)].

[5] L. Blecha, T. J. Cox, A. Loeb, and L. Hernquist, arXiv:1009.4940 [Mon. Not. R. Astron. Soc. (to be published)].

[6] S. Komossa, H. Zhou, and H. Lu, Astrophys. J. **678**, L81 (2008); G. A. Shields, D. J. Rosario, K. L. Smith, E. W. Bonning, S. Salviander, J. S. Kalirai, R. Strickler, E. Ramirez-Ruiz, A. A. Dutton, T. Treu, and P. J. Marshall, Astrophys. J. **707**, 936 (2009); P. G. Jonker, M. A. P. Torres, A. C. Fabian, M. Heida, G. Miniutti, and D. Pooley, Mon. Not. R. Astron. Soc. **407**, 645 (2010); D. Batcheldor, A. Robinson, D. J. Axon, E. S. Perlman, and D. Merritt, Astrophys. J. **717**, L6 (2010); L. Blecha, F. Civano, M. Elvis, and A. Loeb, Mon. Not. R. Astron. Soc. **428**, 1341 (2013); arXiv:1205.6202.

[7] J. G. Baker, J. Centrella, D. Choi, M. Koppitz, J. R. van Meter, and M. C. Miller, Astrophys. J. **653**, L93 (2006); M. Campanelli, C. O. Lousto, Y. Zlochower, and D. Merritt, Astrophys. J. **659**, L5 (2007); J. A. Gonzalez, M. D. Hannam, U. Sperhake, B. Bruegmann, and S. Husa, Phys. Rev. Lett. **98**, 231101 (2007); M. Campanelli, C. O. Lousto,

Y. Zlochower, and D. Merritt, Phys. Rev. Lett. **98**, 231102 (2007); J. G. Baker, W. D. Boggs, J. Centrella, B. J. Kelly, S. T. McWilliams, M. C. Miller, and J. R. van Meter, Astrophys. J. **682**, L29 (2008); B. Bruegmann, J. A. Gonzalez, M. D. Hannam, S. Husaand, and U. Sperhake, Phys. Rev. D **77**, 124047 (2008); C. O. Lousto and Y. Zlochower, Phys. Rev. Lett. **107**, 231102 (2011).

[8] R. Owen *et al.*, Phys. Rev. Lett. **106**, 151101 (2011); D. A. Nichols *et al.*, Phys. Rev. D **84**, 124014 (2011); A. Zimmerman, D. A. Nichols, and F. Zhang, Phys. Rev. D **84**, 044037 (2011).

[9] J. D. Schnittman, A. Buonanno, J. R. van Meter, J. G. Baker, W. D. Boggs, J. Centrella, B. J. Kelly, and S. T. McWilliams, Phys. Rev. D **77**, 044031 (2008).

[10] T. Damour and A. Gopakumar, Phys. Rev. D **73**, 124006 (2006).

[11] P. A. Sundararajan, G. Khanna, and S. A. Hughes, Phys. Rev. D **81**, 104009 (2010).

[12] R. H. Price, G. Khanna, and S. A. Hughes, Phys. Rev. D **83**, 124002 (2011).

[13] R. H. Boyer and R. W. Lindquist, J. Math. Phys. (N.Y.) **8**, 265 (1967).

[14] A. Ori and K. S. Thorne, Phys. Rev. D **62**, 124022 (2000).

[15] A. Buonanno and T. Damour, Phys. Rev. D **62**, 064015 (2000).

[16] J. M. Bardeen, W. H. Press, and S. A. Teukolsky, Astrophys. J. **178**, 347 (1972).